Fluorescence Characterization of Structural Transitions at the Strong Actin Binding Motif in Skeletal Myosin Affinity Labeled at Cysteine 540 with Novel Spectroscopic Cysteaminyl Mixed Disulfides†

Raoul Bertrand, Jean Derancourt, and Ridha Kassab*

Centre de Recherches de Biochimie Macromoléculaire du CNRS, UPR 1086, 1919 Route de Mende, 34293 Montpellier Cedex 5, France

Received April 12, 2000; Revised Manuscript Received September 18, 2000

ABSTRACT: We have synthesized the luminescent and fluorescent lanthanide chelate *S*-(2-nitro-5-thiobenzoic acid)cysteaminyldiethylenetriaminepentaacetate-5-[(2-aminoethyl)amino]naphthalene-1-sulfonic acid as well as the fluorescent analogue *S*-(2-nitro-5-thiobenzoic acid)cysteaminyl-5-carboxyfluorescein using the procedure we recently described [Bertrand, R., Capony, J.-P., Derancourt, J., and Kassab, R. (1999) *Biochemistry 38*, 11914−11925]. Both mixed disulfides react with the skeletal myosin motor domain (S-1) as actin site-directed agents and label exclusively and stoichiometrically Cys 540 in the hydrophobic strong actin binding helix−loop−helix motif, causing only a 1.9−2.4-fold decrease in the V_{max} for acto-S-1 ATPase. The covalently attached cysteaminyl probe side chain spans maximally 17 and 8 Å, respectively, and the fluorophores have different polarity, volume, and flexibility. Thus, they may provide complementary spectroscopic information on the environmental properties of this critical actin binding region. Here, we have analyzed by extrinsic fluorescence spectroscopy S-1 derivatized with the fluorescein label or with the Tb^{3+} or Eu^{3+} chelate of the other label to assess the conformational transitions precisely occurring at this site upon interaction with F-actin, nucleotides, or phosphate analogues. For either label, specific spectral changes of significant amplitude were obtained, identifying at least two major structural states. One was mediated by rigor binding of F-actin in the absence or presence of MgADP. It was abolished by MgATP, and it was not produced by the binding of nonpolymerizable G-actin. A modeling of the corresponding changes in the intensity and λ_{max} of the fluorescence emission spectra, achieved using the fluorescent adducts of 2-mercaptoethanol in varying concentrations of dimethylformamide, illustrates the predicted apolar nature of the strong acto-S-1 interface. A second state was promoted by the binding of ATP, AMP-PNP, ADP·AlF4, ADP·BeFx, or PP_i. It should be prevalent in the weak acto-S-1 binding complexes. The accompanying fluorescence intensity reduction, observed with each label, in both the absence and presence of F-actin, would result from a specific modification by these ligands of the probe orientation and/or solvent accessibility as suggested by acrylamide quenching experiments. It could represent the spectral manifestation of the predicted allosteric linkage from the ATPase site to the strong actin binding site of S-1 that modulates the acto-S-1 affinity. Our study offers the basis necessary for further detailed spectroscopic investigations on the conformational dynamics in solution of the stereospecific and hydrophobic actin binding motif during the skeletal cross-bridge cycle.

Force production in muscle results from the interaction between F-actin and the myosin motor domain or S-1[1] with concomitant ATP hydrolysis. The binding of S-1 to actin is thought to take place in a two-step reaction involving a transition from a weakly and nonstereospecifically attached state to a strongly and stereospecifically bound complex (*1*−*3*). The dynamics of these interactions are strongly influenced by the nucleotides bound at the active site of S-1 which allosterically modulate its affinity for actin. The establishment of the strong, rigor-like bond between S-1 and actin at the end of the cross-bridge cycle is an essential molecular event as it not only enhances the rate of product release at the remote S-1 ATPase site but also seems to contribute

† This research was supported by grants from the Centre National de la Recherche Scientifique and the Association Française contre les Myopathies.

* To whom correspondence and reprints requests should be addressed. Fax: 33 467 52 1559. E-mail: kassab@crbm.cnrs-mop.fr. Tel: 33 4 67 61 33 35.

[1] Abbreviations: S-1, myosin subfragment 1; acto-S-1, actomyosin subfragment 1; ATPase, adenosine-5′-triphosphatase; DTNB, 5,5′-dithiobis(2-nitrobenzoic acid); EDANS, 5-[(2-aminoethyl)amino]naphthalene-1-sulfonic acid; DTPA, diethylenetriaminepentaacetic acid; NTB-cysteaminylcarboxyfluorescein, *S*-(2-nitro-5-thiobenzoic acid)-cysteaminyl-5-carboxyfluorescein; NTB-cysteaminyl-DTPA-EDANS, *S*-(2-nitro-5-thiobenzoic acid)cysteaminyldiethylenetriaminepentaacetate-5-[(2-aminoethyl)amino]naphthalene-1-sulfonic acid; [(cysteaminyl-5-carboxyfluorescein)-Cys]S-1, myosin subfragment 1 modified at cysteine with NTB-cysteaminylcarboxyfluorescein; [(cysteaminyl-DTPA-EDANS)-Cys]S-1, myosin subfragment 1 modified at cysteine with NTB-cysteaminyl-DTPA-EDANS; (cysteaminyl-DTPA-EDANS)-*S*−*S*-(2-mercaptoethanol), model compound 2-mercaptoethanol labeled with NTB-cysteaminyl-DTPA-EDANS; (cysteaminyl-5-carboxyfluorescein)-*S*−*S*-(2-mercaptoethanol), model compound 2-mercaptoethanol labeled with NTB-cysteaminylcarboxyfluorescein; DMF, dimethylformamide; NEM, *N*-ethylmaleimide; $NaDodSO_4$, sodium dodecyl sulfate; MOPS, 3-(*N*-morpholino)propanesulfonic acid.

10.1021/bi000834u CCC: $19.00
Published on Web 11/02/2000

significantly to the generation of mechanical work according to earlier energetic studies (*1*, *4*, *5*) and to more recent resonance energy transfer measurements (*6*). Thus, conformational changes at or near the strong actin binding surface of S-1 would serve both to mediate the cyclical association−dissociation of the acto-S-1 complex and to coordinate the reorientation of the lever arm domain of S-1, thereby facilitating the power stroke (*7*). Structural changes at the acto-S-1 interface were not visualized in the atomic models of the acto-S-1 complex because only the static protein structures were brought together (*8*−*10*). The knowledge of the location, nature, and amplitude of these conformational transitions in solution using different experimental approaches will improve our understanding of the molecular mechanism of energy transduction by the actomyosin−ATP complex.

A major region of the skeletal S-1 that is involved in the tight binding of actin is the hydrophobic helix−loop−helix motif of the heavy chain residues 516−558 residing in the lower 50 kDa subdomain and which interacts with exposed hydrophobic amino acids of the α-helix 338−348 on actin. The conformation of this motif, together with that adopted by the adjacent ordered surface loop of residues 405−415 in the upper 50 kDa subdomain, is thought to control the closure movement of the cleft separating the two 50 kDa subdomains, thereby determining the strength of the acto-S-1 binding during the intermediate stages of the contractile cycle (*11*). Recently, intrinsic tryptophan fluorescence measurements on smooth myosin S-1 mutants including a single tryptophan residue at either of these two parts of the strong actin binding interface were carried out to investigate the structural rearrangements taking place in this region upon interaction of actin or actin + ADP (*12*). In the present work, we extend the fluorescence technique to the native rabbit skeletal S-1, and we probe by extrinsic fluorescence spectroscopy the conformational changes promoted by F-actin and/or nucleotides or phosphate analogues around Cys 540 located at the end of the first helix within the actin binding helix−loop−helix motif. The study was made possible by the remarkable property of two novel luminescent and/or fluorescent cysteaminyl mixed disulfides we have synthesized to be structurally targeted to the hydrophobic strong actin binding site and to label with a high specificity Cys 540 without much affecting the essential S-1 functions. The data describe the environmental changes reported by the two different probes and provide the framework useful for future detailed spectroscopic analyses.

MATERIALS AND METHODS

Chemicals. Cysteamine hydrochloride, 5,5′-dithiobis(2-nitrobenzoic acid) (DTNB), terbium chloride hexahydrate, and europium chloride hexahydrate were obtained from Fluka. Diethylenetriaminepentaacetic dianhydride (DTPA dianhydride) was supplied by Aldrich. 5-Carboxyfluorescein succinimidyl ester and 5-[(2-aminoethyl)amino]naphthalene-1-sulfonic acid sodium salt (EDANS Na^+) were from Molecular Probes (Eugene, OR). *N*-Ethylmaleimide (NEM) was obtained from Sigma. Chymotrypsin and TPCK-treated trypsin were purchased from Worthington.

Proteins. Rabbit skeletal myosin was prepared as described previously (*13*). Chymotryptic S-1 (A1 and A2) was obtained according to ref *14*. F-Actin from rabbit skeletal muscle was prepared by the procedure described in ref *15*. Maleimidobenzoyl-G-actin was prepared as reported earlier (*16*). Protein concentrations were determined spectrophotometrically at 280 nm with an extinction coefficient $A_{1\%}$ of 7.5 cm^{-1} for S-1 (*17*) and 11.0 cm^{-1} for actin (*18*). The concentration of labeled S-1 derivatives was calculated after subtracting the absorbance of the modifying group at this wavelength. For each S-1 preparation, the labeling ratios were measured spectrophotometrically using the following molar extinction coefficients: EDANS = 5900 M^{-1} cm^{-1} at 337 nm and carboxyfluorescein = 74000 M^{-1} cm^{-1} at 494 nm. The labeling stoichiometry was 1.0−1.1 and 0.80−0.95 for S-1 conjugated to EDANS and to carboxyfluorescein, respectively. The concentration of free nitrothiobenzoate ion was estimated at 412 nm using a molar extinction coefficient of 14150 M^{-1} cm^{-1} (*19*).

Synthesis Reactions. The two spectroscopic cysteaminyl mixed disulfides were prepared using the two-step experimental strategy we recently described for the synthesis of *S*-(2-nitro-5-thiobenzoic acid)cysteaminyl-EDTA (NTB-cysteaminyl-EDTA) (*20*). It essentially involves the quantitative disulfide−thiol exchange reaction in aqueous medium between DTNB and cysteamine, followed by the substitution of the amino group in the resulting *S*-(2-nitro-5-thiobenzoic acid)cysteamine (NTB-cysteamine) with the side chain carrying the spectroscopic probe.

(a) Synthesis of S-(2-Nitro-5-thiobenzoic acid)cysteaminyl-DTPA-EDANS (NTB-Cysteaminyl-DTPA-EDANS). Cysteamine hydrochloride (11 mM) in 500 mM MOPS (pH 8.5) was reacted for 30 min at 20 °C with a 1.1-fold molar excess of DTNB dissolved in dimethylformamide (620 mM). To the NTB-cysteamine-containing solution, EDANS Na^+ (25 mM), dissolved in 25 mM NaOH by heating at 60 °C, was added to a final concentration of 7 mM. DTPA dianhydride (150 mM), dissolved in dimethylformamide by heating at 80 °C, was then immediately added under vigorous stirring, to a final concentration of 26 mM, using six equal aliquots each introduced after an interval of 10 min. The NTB-cysteaminyl-DTPA-EDANS conjugate that formed was isolated by reverse-phase HPLC using essentially the standard chromatographic conditions employed for the isolation of NTB-cysteaminyl-EDTA (*20*). It was eluted as a single peak at 27% acetonitrile. The chemical structure of the fluorescent mixed disulfide was confirmed by ionization mass spectrometry, which revealed a unique product with a molecular mass of 899.95 Da (calculated mass of 897.94). Its concentration was determined spectrophotometrically at 412 nm after incubation in 50 mM Tris-HCl (pH 8.0) containing 1 mM 2-mercaptoethanol for 1 h at 20 °C. This assay indicated that at least 20% of the starting cysteamine was recovered as NTB-cysteaminyl-DTPA-EDANS. The bulk of the purified material accumulated after several chromatographic runs was fractionated into 1 mL aliquots, which were dried with a Speed Vac centrifuge and stored at −20 °C.

(b) Synthesis of S-(2-Nitro-5-thiobenzoic acid)cysteaminyl-5-carboxyfluorescein (NTB-Cysteaminylcarboxyfluorescein). The NTB-cysteamine precursor was first isolated by subjecting 75 μL aliquots of the corresponding mixture to reverse-phase HPLC as described (*20*). It was eluted as a single peak at 18% acetonitrile. After several similar chromatographic runs, the pooled fractions were dried as indicated above and

stored at −20 °C. The dry material was dissolved in 100 mM MOPS (pH 8.5) at a final concentration of 1 mM, and its concentration was measured spectrophotometrically at 412 nm. 5-Carboxyfluorescein succinimidyl ester (15 mM) dissolved in dimethylformamide was then added to a final concentration of 1.5 mM. After 3 h at 4 °C, 300 μL aliquots were submitted to reverse-phase HPLC as described (*20*). The NTB-cysteaminylcarboxyfluorescein was eluted at 47% acetonitrile with no trace of residual NTB-cysteamine in the chromatographic profile. It was dried and stored at −20 °C. About 80% of the starting cysteamine was recovered as the fluorescent cysteaminyl mixed disulfide as assessed by the spectrophotometric assay at 412 nm.

Derivatization of S-1. S-1 (40−50 μM) in 20 mM MOPS (pH 8.0) was mixed with a 1.1−1.5-fold molar excess of NTB-cysteaminyl-DTPA-EDANS or NTB-cysteaminylcarboxyfluorescein, dissolved immediately before use in 50 mM Tris-HCl (pH 7.2) at a concentration of 250 mM. The reaction was monitored at 412 nm for 120 and 90 min at 20 °C, respectively. The concentration of the released nitrothiobenzoate ion was estimated at 412 nm. In parallel, protein aliquots were withdrawn at various time intervals and subjected to ATPase measurements. The labeled proteins were isolated by gel filtration over a PD 10 column equilibrated in 50 mM MOPS (pH 7.5). The [(cysteaminyl-DTPA-EDANS)-Cys]S-1 derivative (25 μM) was incubated with a 1.5-fold molar excess of $TbCl_3$ or $EuCl_3$, dissolved in water at a concentration of 1 mM, for 2 h at 4 °C, and the chelate was then purified on a PD 10 column in 50 mM MOPS (pH 7.5). 2-Mercaptoethanol was labeled by reacting either fluorescent mixed disulfide reagent with a 100−200-fold molar excess of the thiol compound in 50 mM MOPS (pH 7.5) for 1 h at 20 °C.

Identification of the Site of Fluorophore Attachment in S-1. S-1 (40 μM) in 20 mM MOPS (pH 8.0) was treated at 20 °C with a 1.5-fold molar excess of NTB-cysteaminyl-DTPA-EDANS for 120 min or with a 1.2-fold molar excess of NTB-cysteaminylcarboxyfluorescein during 90 min. The pH of the solution was then brought to 7.5 by adding MOPS (500 mM, pH 7.0) to a final concentration of 50 mM. NEM dissolved in dimethyformamide (250 mM) was added to each mixture at a 5-fold molar excess over total S-1 thiols. After 15 min at 20 °C, the temperature of the solutions was lowered to 0 °C in an ice bath, and $NaDodSO_4$ (10% in water) was added to a final concentration of 0.5%. After 20 min at 0 °C, the modified S-1 was gel filtered over a NAP-10 column (Pharmacia) eluted at 20 °C with 50 mM MOPS and 0.01% $NaDodSO_4$ (pH 8.0). One milliliter of the labeled S-1 preparation (25 μM) was digested at 37 °C for 2 h with chymotrypsin at an enzyme:substrate weight ratio of 1:10. Each digest was fractionated by reverse-phase HPLC on an Aquapore C-8 Brownlee RP-300 column (4 × 220 mm) eluted for 60 min with a linear gradient of 0−100% solvent B consisting of 75% acetonitrile in 0.1% aqueous trifluoroacetic acid (solvent A), at a flow rate of 1 mL/min. The absorbance of the effluent was monitored at 220 nm. The fluorescent fractions were detected after illumination of aliquots, the pH of which was adjusted to 8.0, with a long-wavelength ultraviolet light. They were pooled and further purified on a Brownlee Spheri-5 RP C-18 column (4.6 × 220 mm) eluted for 40 min with 50−100% solvent B consisting of 75% acetonitrile in 0.1% trifluoroacetic acid (solvent A), under the same conditions. A final purification of the fluorescent fractions was achieved using a Brownlee C-18 column (2 × 100 mm) eluted for 40 min with 20−60% solvent B consisting of 95% acetonitrile in 0.1% trifluoroacetic acid and 0.005% trimethylamine (solvent A), at a flow rate of 200 μL/min and collecting 200 μL fractions.

Amino acid sequencing of the pure fluorescent peptides was conducted using a Perkin-Elmer Procise 492 sequencer operating according to the manufacturer's pulsed liquid program. Mass values were determined by electrospray ionization mass spectrometry on a VG trio-2000 mass spectrometer as previously described (*20*).

Fluorescence Measurements. The fluorescence experiments were performed at 20 °C using a Kontron Bio-Tek spectrometer (Photon Technology International). The employed buffer was 50 mM MOPS (pH 7.5). Corrected fluorescence emission spectra were recorded for S-1 (2 μM) labeled with either EDANS or carboxyfluorescein at 400−575 nm (excitation at 337 nm; 4 nm slit width) and 500−550 nm (excitation at 494 nm; 1 nm slit width), respectively. A 1 nm band-pass was used for all samples. The quenching of fluorescence by varying concentrations of acrylamide (0−150 mM) was employed to assess the accessibility of the fluorophores to solvent. The results were presented as Stern−Volmer plots to estimate the quenching constant K_{sv} (*21*). Fluorescence emisson spectra of probe-labeled 2-mercaptoethanol at various ratios of dimethylformamide/water were recorded as described for labeled protein.

ATPase Assays. The Ca^{2+}-ATPase activities were measured at 25 °C in the presence of 2.5 mM ATP, 250 mM KCl, 5 mM $CaCl_2$, and 50 mM Tris-HCl (pH 7.7). The K^+-EDTA ATPase activities were determined at 25 °C in 2.5 mM ATP, 1 M KCl, 5 mM EDTA, and 50 mM Tris-HCl (pH 7.5). The acto-S-1 ATPase was assayed at 25 °C in a medium (1 mL) containing 5 mM ATP, 2.5 mM $MgCl_2$, 10 mM KCl, and 50 mM Tris-HCl (pH 8.0) using 1.0 mg of F-actin and 50 μg of S-1. The actin-activated ATPase activities were also measured under similar conditions in the presence of varying concentrations (0.8−3.3 mg/mL) of F-actin. Inorganic phosphate was estimated colorimetrically as described (*22*).

Electrophoresis. $NaDodSO_4$−polyacrylamide gradient gel electrophoresis (5−18%) was carried out as previously described (*22*, *23*) except that the pH of the Laemmli buffer was 7.5 and β-mercaptoethanol was omited. Fluorescent bands were located in the gels by illumination with a long-wavelength ultraviolet light before staining with Coomassie blue.

RESULTS

Actin Site-Directed Labeling of S-1 with the Spectroscopic Cysteaminyl Mixed Disulfides. NTB-cysteaminyl-DTPA-EDANS and NTB-cysteaminylcarboxyfluorescein were easily generated in aqueous medium via the simple synthesis pathway, schematically depicted in Figure 1A and which we recently employed for the production of the nonspectroscopic analogue NTB-cysteaminyl-EDTA (*20*). The latter mixed disulfide was found to undergo a selective reaction with Cys 540 in the primary hydrophobic strong actin binding helix−loop−helix motif of residues 516−558 of skeletal S-1. The

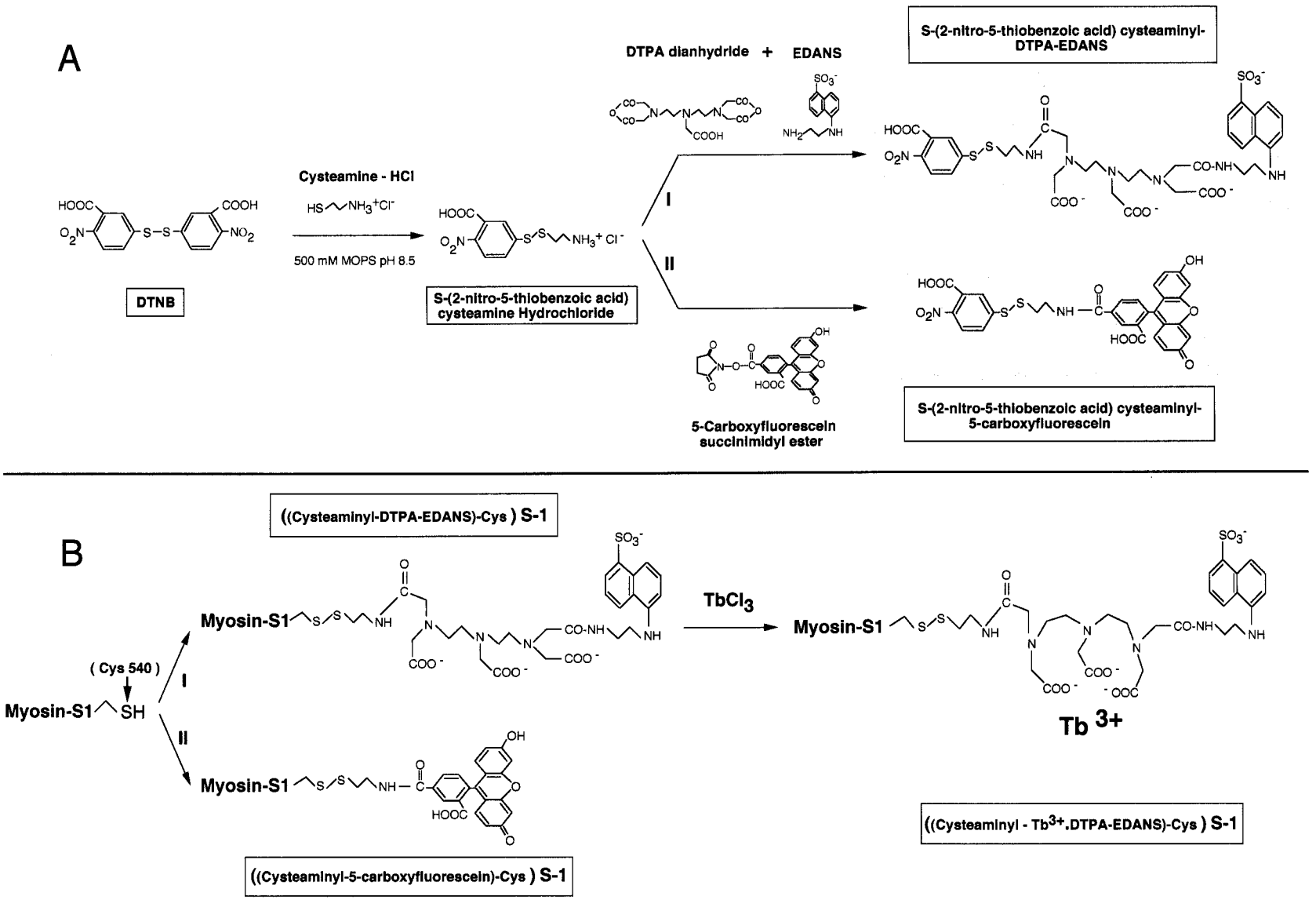

FIGURE 1: Reaction pathways for the synthesis of the spectroscopic cysteaminyl mixed disulfides NTB-cysteaminyl-DTPA-EDANS (AI) and NTB-cysteaminylcarboxyfluorescein (AII) and for their subsequent conjugation to S-1 to form the luminescent and fluorescent chelate [(cysteaminyl-Tb^{3+}·DTPA-EDANS)-Cys]S-1 (BI) or the fluorescent derivative [(cysteaminylcarboxyfluorescein)-Cys]S-1 (BII).

Fe^{3+} chelate of the disulfide-bridged cysteaminyl-EDTA side chain served to assess, by a limited and site-specific chemical proteolysis of the S-1 heavy chain, the F-actin- and/or nucleotide-mediated conformational changes at the adjacent switch II helix (*20*). In particular, our data pointed out the ability of the negatively charged EDTA moiety to direct the disulfide−thiol exchange process to Cys 540 without modification of any other thiol of the S-1 heavy chain. However, a partial secondary derivatization of S-1 did also take place at the single cysteine of the alkali light chains. For the two new spectroscopic mixed disulfides, chemical structural features were designed within the cysteaminyl probe side chain to maximize the reaction specificity toward Cys 540 and to avoid the substitution of the alkali light chain thiol. Thus, in addition to the carboxyl groups, an aromatic dye, such as EDANS or fluorescein, was introduced. These two chromophores were selected not only because they are well-known environmentally sensitive reporter groups but also because their hydrophobic character was expected to complement the apolar residues of the strong actin binding motif further targeting the mixed disulfides to Cys 540. In this regard, earlier, the succinimidyl ester of carboxyfluorescein was shown to selectively acylate Lys 553 residing at the end of the actin binding motif (*22*, *24*). Following the proposed actin site-directed labeling reaction between S-1 and either of the two disulfide agents (Figure 1B), the corresponding S-1 derivatives that formed could serve for fluorescence studies and in the case of the DTPA-EDANS-labeled S-1 for luminescence measurements as well after chelation of Tb^{3+} or Eu^{3+} to the protein-bound DTPA group (*25*, *26*). An additional advantage of the dual S-1 labeling is that the EDANS and carboxyfluorescein labels are connected to the Cα of cysteine by different arm lengths corresponding to about 17 and 8 Å, respectively. Therefore, they offer the potential to monitor the local environmental characteristics at different distances from Cys 540. Moreover, their spectroscopic information could be complementary as the two fluorophores also differ in their physicochemical properties such as polarity, size, and flexibility.

To demonstrate the suitability of the S-1 conjugates for spectroscopic investigations, we have first estimated the stoichiometry of the labeling reactions, determined whether Cys 540 is the unique site in the S-1 molecule serving for the incorporation of each probe, and evaluated the impact of each bound cysteaminyl probe side chain on the major enzymatic functions of S-1. As illustrated in Figure 2, the treatment of S-1, at pH 8.0 and room temperature, with a 1.5-fold molar excess of either NTB-cysteaminyl-DTPA-EDANS (Figure 2A) or NTB-cysteaminylcarboxyfluorescein (Figure 2B) resulted in the progressive incorporation of about 1.10 and 0.95 mol of label/mol of S-1, respectively, as determined by spectrophotometric measurements at 412 nm of the amount of 2-nitro-5-thiobenzoate anion that was released. Extensive labeling of S-1 also occurred even when the protein was reacted with an equimolar amount of either disulfide reagent since 1.0 mol of EDANS and 0.80 mol of carboxyfluorescein/mol of S-1 were found attached to the protein by direct spectrophotometric analyses on the S-1 derivatives isolated after 120 and 90 min labeling reaction, respectively. Thus, an almost complete and stoichiometric labeling of S-1 could be achieved with the two spectroscopic mixed disulfides tested. The nucleotides, ATP or ADP, and

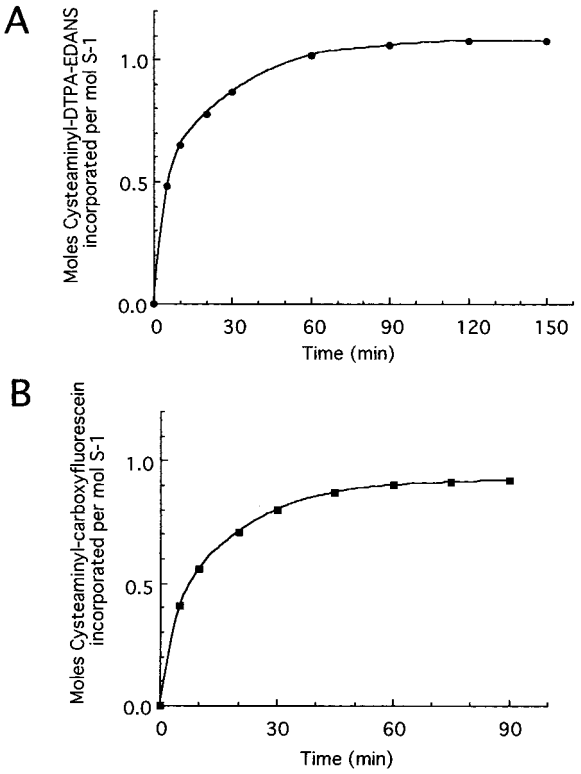

FIGURE 2: Time course of the stoichiometric incorporation of the cysteaminyl-DTPA-EDANS group or the cysteaminylcarboxyfluorescein group into myosin S-1. The protein (10 μM) in 20 mM MOPS (pH 8.0) was reacted at 20 °C with a 1.5-fold molar excess of NTB-cysteaminyl-DTPA-EDANS (A) or NTB-cysteaminylcarboxyfluorescein (B). The extent of S-1 modification during each disulfide−thiol exchange process was estimated by spectrophotometric measurements at 412 nm of the amount of nitrothiobenzoate ion released.

the phosphate analogues, AMPPNP or PP_i, added at millimolar concentrations did not noticeably change the rate or the extent of any modification reaction. The effect of F-actin binding to S-1 could not be defined because a parallel reaction of the disulfides with actin was also observed. Figure 3 shows that the limited tryptic digestion of each labeled S-1 preparation gives rise to the same electrophoretic profile as native S-1, suggesting that no gross conformational changes have occurred in S-1 by the labeling. The fluorescence of EDANS (panel B, lane b) or carboxyfluorescein (panel C, lane b) was associated only with the central tryptic 50 kDa heavy chain fragment, and no label incorporation into the alkali light chains A1 and A2 was apparent (panel A, lane a). The latter important observation was confirmed by subjecting either labeled S-1 sample to reverse-phase HPLC under the experimental conditions we reported previously (*18*, *20*), which permit the separation of the 95 kDa heavy chain from the alkali light chains. Their measured fluorescence profile indicated unambiguously that each S-1 label was bound only to the heavy chain fractions (data not shown). On the basis of these findings, each labeled S-1 was directly alkylated with NEM and extensively digested with chymotrypsin. The generated peptides were then fractionated by reverse-phase HPLC. A single pure fluorescent peptide was isolated from either labeled S-1. After 20 cycles of Edman degradation reactions, the microsequencing of the EDANS-labeled peptide identified the sequence between Ser 534 and Lys 553 of the S-1 heavy chain. For the carboxy-

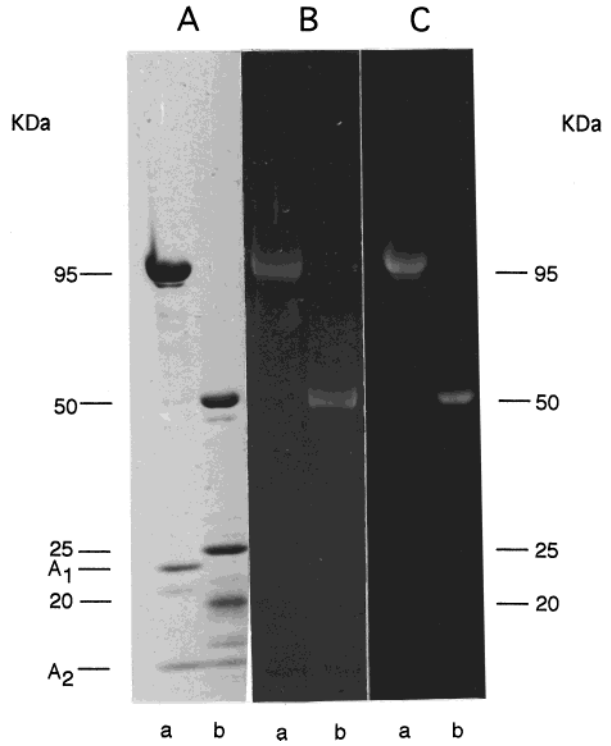

FIGURE 3: Electrophoretic identification of the S-1 heavy chain fragment labeled with cysteaminyl-DTPA-EDANS (panel B) or cysteaminylcarboxyfluorescein (panel C). Samples of purified labeled S-1 (20 μM) in 20 mM MOPS (pH 8.0) (lanes a) were treated with trypsin at a protease to substrate weight ratio of 1:50. After 20 min at 25 °C, the proteolysis was quenched by mixing a protein aliquot with boiling Laemmli buffer (pH 7.5) in the absence of β-mercaptoethanol. The digests were then subjected to Na-DodSO$_4$ gel electrophoresis using a 5−18% gradient acrylamide gel, and fluorescent bands were viewed under UV light (lanes b). The Coomassie blue-stained electrophoretograms of labeled S-1 before and after digestion are shown in panel A. Each fluorophore was incorporated exclusively into the central tryptic 50 kDa fragment.

fluorescein-derivatized peptide, 10 cycles revealed the sequence between Leu 536 and Ala 545. In the determined sequence of each peptide there was only one gap corresponding to Cys 540 of the heavy chain sequence. These data unequivocally indicate that this residue represents the unique site for the covalent attachment of either cysteaminyl probe side chain within the entire S-1 molecule. They also ascertain the idea that the spectroscopic responses of each probe will originate only from the region around Cys 540.

The influence of the derivatization of this residue on the S-1 enzymatic activities during the entire course of each disulfide−thiol exchange reaction is presented in Figure 4, using a molar ratio of NTB-cysteaminyl-DTPA-EDANS (Figure 4A) or NTB-cysteaminylcarboxyfluorescein (Figure 4B) to S-1 of 1.5. The incubation of S-1 with the former reagent for 150 min did not alter the K^+- or Ca^{2+}-ATPase activities whereas the acto-S-1 ATPase did undergo a progressive inhibition and plateaued at about 40% of the control. This 60% extent of inactivation is obviously correlated with a complete substitution of Cys 540. Earlier, the reaction of NTB-cysteaminyl-EDTA, under the same conditions, was found to affect quite similarly the enzymatic properties of S-1 (*20*). The conjugation of S-1 to cysteaminylcarboxyfluorescein also promoted the decrease of the acto-S-1 ATPase to about 45% of the control. This effect was

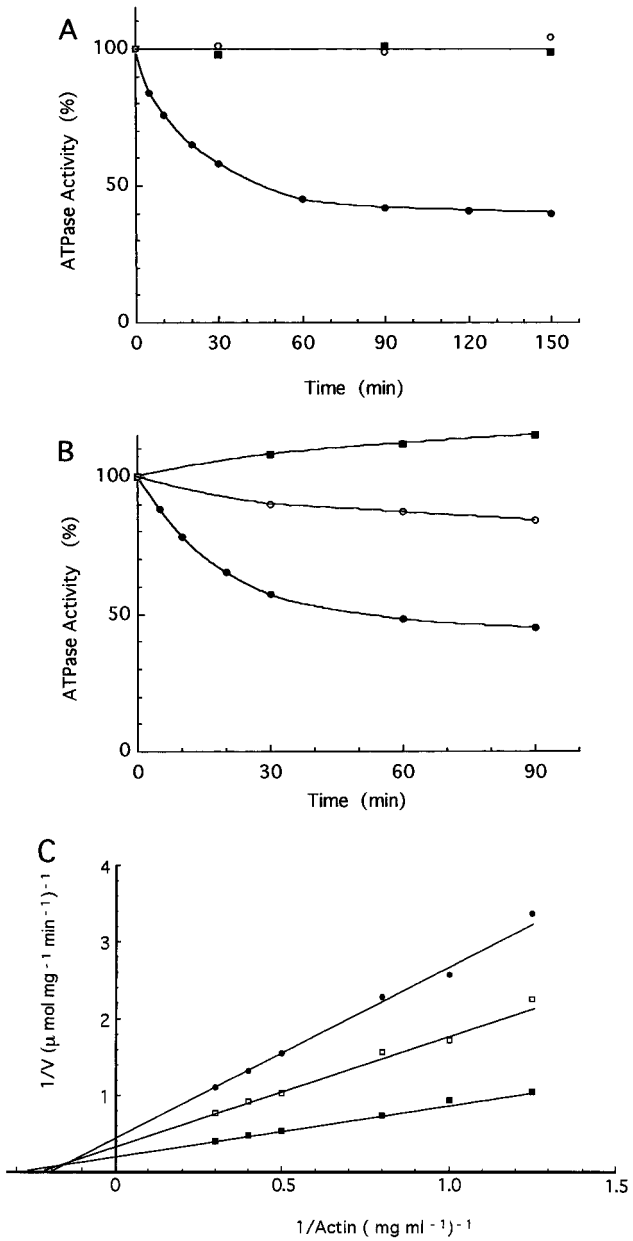

FIGURE 4: Selective inhibition of the acto-S-1 ATPase upon substitution of S-1 with cysteaminyl-DTPA-EDANS or cysteaminylcarboxyfluorescein. S-1 (50 μM) was incubated at 20 °C in 20 mM MOPS (pH 8.0) with a 1.5-fold molar excess of NTB-cysteaminyl-DTPA-EDANS (A) or NTB-cysteaminylcarboxyfluorescein (B). At the indicated time intervals, protein samples were withdrawn and assayed for K^+-ATPase (○), Ca^{2+}-ATPase (■), and actin-activated ATPase (●). (C) Double-reciprocal plots of the amount of activated Mg^{2+}-ATPase of [(cysteaminyl-DTPA-EDANS)-Cys]S-1 (●), [(cysteaminylcarboxyfluorescein)-Cys]S-1 (□), and native S-1 (■) as a function of actin concentration (0.8−3.3 mg/mL). All of the enzymatic activities were measured as described in Materials and Methods.

accompanied by a 15% reduction of the K^+-ATPase and an equal enhancement of the Ca^{2+}-ATPase. The slight change in these two ATPases is most likely resulting from a specific communication between the ATPase site and the aromatic carboxyfluorescein group attached to Cys 540 in the strong actin binding site. Earlier, the binding of this group to the proximal Lys 553 was also found to change some of the actin-independent S-1 ATPases (*22*). Double-reciprocal plots of the actin-activated ATPases of native S-1 and S-1 substituted with either fluorescent disulfide (Figure 4C and

Table 1: Kinetic Parameters of [(Cysteaminyl-DTPA-EDANS)-Cys]S-1 and [(Cysteaminylcarboxyfluorescein)-Cys]S-1[a]

proteins	K_m (μM)	V_{max} (s^{-1})
native S-1	90 ± 4	10.8 ± 0.3
[(cysteaminyl-DTPA-EDANS)-Cys]S-I	110 ± 12	4.4 ± 0.5
[(cysteaminylcarboxyfluorescein)-Cys]S-1	97 ± 8	5.6 ± 0.4

[a] Acto-S-I ATPase assays were conducted as described in Materials and Methods in the presence of varying concentrations of F-actin for native S-1 (control), S-1 containing 1.1 mol of bound cysteaminyl-DTPA-EDANS, and S-1 containing 0.95 mol of bound cysteaminyl-carboxyfluorescein/mol of protein. V_{max} and K_m values were calculated from double-reciprocal plots of the acto-S-1 ATPases as a function of actin concentration (0.8−3.3 mg/mL), and linear regression analysis was used to fit the data.

Table 1) indicated no change in the K_m for actin whereas the V_{max} value for the labeled S-1 was reduced 2.4-fold in the case of [(cysteaminyl-DTPA-EDANS)-Cys]S-1 and 1.9-fold for [(cysteaminylcarboxyfluorescein)-Cys]S-1. Previously, [(cysteaminyl-EDTA)-Cys]S-1 also showed only a 2.5-fold decrease of the V_{max} of its actin-activated ATPase (*20*). Thus, the moderate reduction of the maximum rate of the acto-S-1 ATPase reaction with little or no alteration of the other S-1 ATPases can be considered, in general, as the signature of Cys 540 labeling by all the cysteaminyl mixed disulfides we have employed. The total activity (V_{max}/K_m) of the two former fluorescently labeled S-1s was 30% and 48%, respectively, of that displayed by native S-1. For comparison, the total activity reported for the tryptophan mutants of the smooth myosin motor domain that served for intrinsic fluorescence analyses of the strong actin binding site was 30−35% of the wild-type protein (*12*). Collectively, our data characterizing the stoichiometric labeling of S-1 at only Cys 540 with a limited impairment of the essential S-1 enzymatic functions strongly suggest that the protein derivatives we obtained are valuable for further spectroscopic studies.

Fluorescence Properties of the Labeled S-1 Derivatives and of Their Complexes with F-Actin. The fluorescence emission spectra of S-1 labeled with the cysteaminyl-Tb^{3+}·DTPA-EDANS chelate or cysteaminylcarboxyfluorescein are displayed in panels A and B of Figure 5, respectively. The stable ligation of the lanthanides, Tb^{3+} or Eu^{3+}, to the DTPA group in the former derivative before the spectral analyses was necessary to avoid the complexation of this group to Mg^{2+}, which was employed in most experiments. As previously observed for other DTPA-lanthanide chelates (*25*), Tb^{3+} induced only a modest fluorescence quenching (about 25%) whereas Eu^{3+} caused 85% reduction of the fluorescence intensity. Thus, for routine work, the terbium complex was employed. The EDANS-labeled S-1 exhibited a maximum fluorescence intensity centered around 472 nm. This intensity magnitude was identical to that observed for the model compound, (cysteaminyl-Tb^{3+}·DTPA-EDANS)-*S*−*S*-(2-mercaptoethanol), but the peak position was 6 nm blue shifted. On the other hand, the maximum fluorescence intensity at 517 nm of carboxyfluorescein-labeled S-1 was reduced by 20%, and the peak position was 2 nm red shifted as compared to the corresponding labeled model derivative of 2-mercaptoethanol. From our model studies concerning the response of the fluorophore labels toward polarity changes (Tables 2 and 3), the fluorescence characteristics of both S-1 derivatives

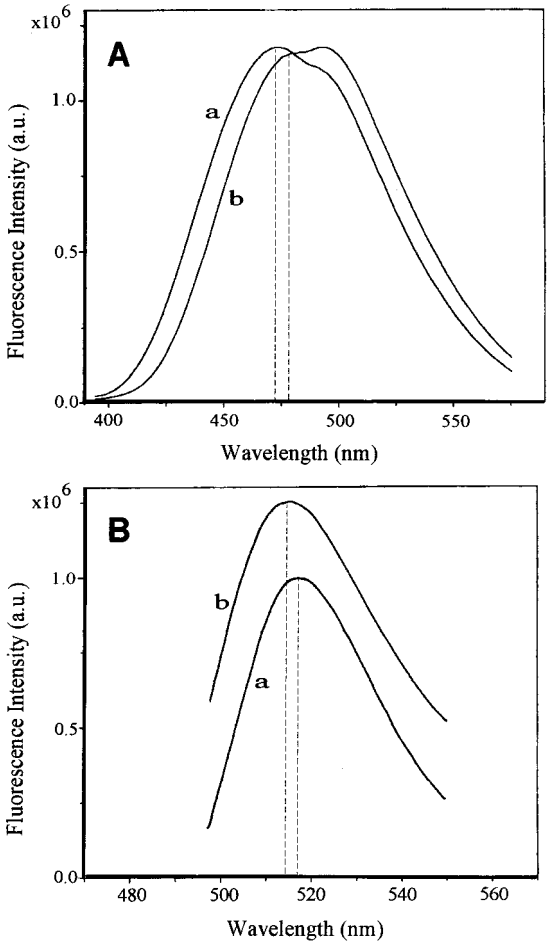

FIGURE 5: Fluorescence emission spectra of [(cysteaminyl-Tb^{3+}·DTPA-EDANS)-Cys]S-1 (Aa) and [(cysteaminylcarboxyfluorescein)-Cys]S-1 (Ba). The spectra of the proteins were measured as indicated in Materials and Methods and were compared with the fluorescence emission spectra of the corresponding labeled model derivatives, (cysteaminyl-Tb^{3+}· DTPA-EDANS)-*S*−*S*-(2-mercaptoethanol) (Ab) and (cysteaminylcarboxyfluorescein)-*S*−*S*-(2-mercaptoethanol) (Bb). The protein or model compound concentration was 2 μM. The emission peak maxima are indicated by straight lines.

suggest that their labels are less exposed to solvent and have a specific environment including apolar components. The limited tryptic digestion of the S-1 derivatives with cleavage of the heavy chain into its three tryptic fragments did not alter the fluorescence spectra. However, the treatment of the proteins with 0.4% $NaDodSO_4$ elicited large fluorescence changes, which resulted from protein unfolding as the denaturation agent had no direct effect on the fluorescence spectra of the probes bound to 2-mercaptoethanol. Thus, the fluorescence spectra observed for the two labeled S-1s reflect the native protein structure.

The binding of F-actin to [(cysteaminyl-Tb^{3+}·DTPA-EDANS)-Cys]S-1 at a 1:1 molar ratio induced the typical fluorescence spectrum displayed in Figure 6. The maximum emission wavelength was further blue shifted from 472 to 466 nm with a 9% increase in the peak intensity. The fluorescence enhancement was larger (18%) with the labeled S-1 chelated to Eu^{3+} (Table 2, part A). These spectral changes were not at all apparent upon the addition of the monomeric G-actin derivative, maleimidobenzoyl-G-actin, although this protein does bind to S-1 at the positively charged 50 kDa−20 kDa loop of the heavy chain (*16*). Thus,

Table 2: Effect of the Environment on the Fluorescence Properties of DTPA-EDANS-Labeled Derivatives[a]

part A			part B		
	λ_{max} (±1 nm)	enhancement of fluorescence intensity (%)		λ_{max} (±1 nm)	enhancement of fluorescence intensity (%)
[(cysteaminyl-Eu^{3+}·DTPA-EDANS)-Cys]S-1			(cysteaminyl-Eu^{3+}·DTPA-EDANS)-*S*−*S*-(2-mercaptoethanol)		
labeled S-1	472		in water	478	
labeled S-1 + F-actin	466	18	+10% DMF	476	42
			+20% DMF	475	80
			+30% DMF	472	105
			+40% DMF	469	150
			+50% DMF	465	190
			+60% DMF	461	250
[(cysteaminyl-Tb^{3+}·DTPA-EDANS)-Cys]S-1			(cysteaminyl-Tb^{3+}·DTPA-EDANS)-*S*−*S*-(2-mercaptoethanol)		
labeled S-1	472		in water	478	
labeled S-1 + F-actin	466	9	+10% DMF	475	20
			+20% DMF	474	40
			+30% DMF	471	60
			+40% DMF	468	75
			+50% DMF	465	95
			+60% DMF	462	115

[a] The fluorescence emission spectra of the Tb^{3+} or Eu^{3+} chelate of the labeled S-1 derivative (2 μM) in 50 mM MOPS and 2 mM $MgCl_2$ (pH 7.5) were measured as indicated under Materials and Methods (part A) and compared with the emission spectra obtained for the corresponding chelates of the labeled model derivative of 2-mercaptoethanol at different ratios of dimethylformamide (DMF)/water (part B).

Table 3: Effect of the Environment on the Fluorescence Properties of Carboxyfluorescein-Labeled Derivatives[a]

part A			part B		
	λ_{max} (±1 nm)	quenching of fluorescence intensity (%)		λ_{max} (±1 nm)	quenching of fluorescence intensity (%)
[(cysteaminylcarboxyfluorescein)-Cys)S-1			(cysteaminylcarboxyfluorescein)-*S*−*S*-(2-mercaptoethanol)		
labeled S-1	517		in water	515	
labeled S-1 + F-actin	519	36	+10% DMF	518	7
			+20% DMF	520	11
			+30% DMF	522	16
			+40% DMF	523	23
			+50% DMF	525	29
			+60% DMF	526	36

[a] The fluorescence emission spectra of the labeled S-1 derivative (2 μM) in 50 mM MOPS and 2 mM $MgCl_2$ (pH 7.5) were measured as indicated under Materials and Methods (part A) and compared with the emission spectra obtained for the corresponding labeled model derivative of 2-mercaptoethanol at different ratios of dimethylformamide (DMF)/water (part B).

the F-actin-induced spectral effects were specific of the polymerized state of actin and were caused by its direct interaction with the strong actin binding motif and not with the other weak actin binding sites. This proposal implies that the association, if any, of the strong actin binding site of S-1 with the monomeric G-actin is negligible. Because the concentration of F-actin employed was low (2 μM), the fluorescence measurements were also performed with phalloidin-stabilized F-actin. The same spectrum was recorded as in the absence of phalloidin (data not shown), indicating that the observed spectral changes were promoted by fully polymerized F-actin under the employed experimental conditions. The complexation of the second S-1 derivative, [(cysteaminylcarboxyfluorescein)-Cys]S-1, to increasing concentrations of F-actin (Figure 7A) resulted in up to 36% quenching of the fluorescence intensity, and the emission maximum was further red shifted from 517 to 519 nm. This large fluorescence decrease allowed an easy titration of the F-actin binding to the labeled S-1 (Figure 7A, inset). The data show that the fluorescence change is concentration dependent and saturable, suggesting a specific binding of F-actin to the S-1 derivative resulting in an altered environment of the fluorescent probe, and after fitting the data to a binding curve, a dissociation constant, K_d, of 1.7 μM ± 0.2 was calculated for this complex. Thus, the rigor binding affinity of the carboxyfluorescein-labeled S-1 for actin was at least 15-fold weaker as compared to the native acto-S-1 assuming a K_d of at least 0.1 μM for the latter complex, under the experimental conditions employed.

The comparison of all the fluorescence measurements for the two labeled S-1 derivatives, used alone or complexed to F-actin, with the fluorescence properties of the corresponding labeled adducts of 2-mercaptoethanol in various concentrations of dimethylformamide is presented in Table 2, parts A and B, and in Table 3, parts A and B. The 6 nm blue shift of the F-actin complex with [(cysteaminyl-Tb^{3+}/Eu^{3+}·DTPA-EDANS)-Cys]S-1 suggests the transfer of the label to a milieu that is equivalent to the polarity of 30−35% dimethylformamide in water. The 36% decrease of the fluorescence intensity of the F-actin complex with [(cysteaminylcarboxyfluorescein)-Cys]S-1 would indicate an environment of the probe that is even more apolar (60% dimethylformamide in

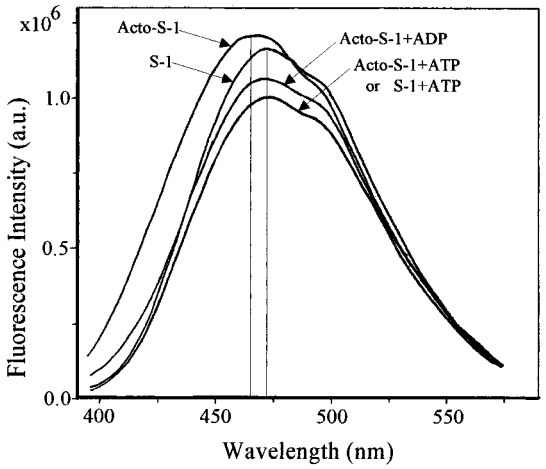

FIGURE 6: Changes in the fluorescence emission spectrum of [(cysteaminyl-Tb^{3+}· DTPA-EDANS)-Cys]S-1 (2 μM) in 50 mM MOPS and 2 mM $MgCl_2$ (pH 7.5) upon binding to F-actin (2 μM) and upon the addition of ATP or ADP (2 mM) to the acto-S-1 derivative complex or the addition of ATP to the S-1 derivative alone. The spectra were collected as specified in Materials and Methods. All data are corrected for dilutions.

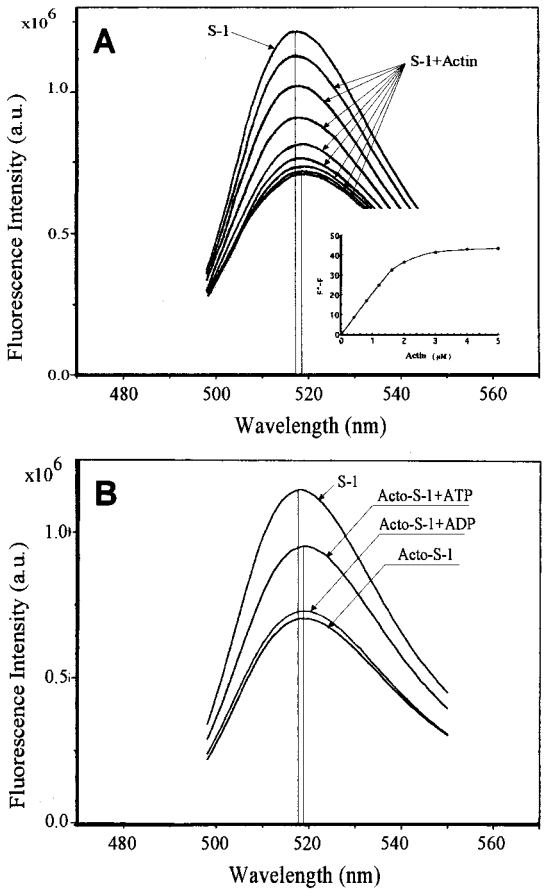

FIGURE 7: (A) F-actin-dependent changes in the fluorescence emission spectrum of [(cysteaminylcarboxyfluorescein)-Cys]S-1 (2 μM) in 50 mM MOPS and 2 mM $MgCl_2$ (pH 7.5). The spectra were measured using increasing concentrations of F-actin (0−5 μM). Inset: the amount of fluorescence intensity decrease ($F_0 - F$) was plotted as a function of actin concentration. (B) The emission spectra recorded for the S-1 derivative (2 μM) in complex with F-actin (2 μM) before and after the addition of ATP or ADP (2 μM) are indicated. All measurements are corrected for dilutions.

water). The latter polarity estimation would be consistent with the positioning of the fluorophore closer to the hydrophobic acto-S-1 interface since the length of its linker arm is shorter.

Nucleotide- and Phosphate Analogue-Induced Fluorescence Changes in the Labeled S-1 Derivatives. We assessed the influence of nucleotides or phosphate analogues on the emission spectra of the two labeled S-1s used in the presence or absence of F-actin. In control experiments employing the labeled conjugates of 2-mercaptoethanol, we verified that the required presence of Mg^{2+} ions had no effect on the fluorescence spectrum of either probe. As shown in Figure 6, the mixing of ATP (2 mM) with EDANS-labeled S-1 (2 μM) complexed with F-actin (2 μM) did not restore the initial fluorescence spectrum of the S-1 derivative but rather it induced a novel spectrum with a maximum emission at 472 nm and a 10% decrease of the fluorescence intensity as compared to the spectrum of S-1 alone. This fluorescence measurement was also performed using higher protein concentrations which favor ternary acto-S-1−nucleotide complex formation. With 7 μM S-1 derivative (labeled at 20%) and 30 μM actin (the analysis was not practicable at a higher actin concentration), essentially the same extent of fluorescence quenching by ATP was recorded as in the presence of the lower actin concentration (data not shown). By contrast, the addition of high NaCl concentrations (>50 mM) to the acto-S-1 derivative complex in the absence of ATP did restore the initial spectrum of the S-1 derivative as a result of its decreased affinity for actin (data not shown). Thus, the ATP-induced spectrum should correspond to the production of a specific binary S-1 derivative−ATP/ADP·P_i complex weakly bound to actin. Furthermore, the addition of ADP led also to a distinct spectrum whose pattern was intermediate as compared to the acto-S-1 and acto-S-1−ATP spectra. It should be related to another specific S-1 derivative−ADP complex less strongly bound to actin than the rigor complex without nucleotide. Similar specific ATP- or ADP-dependent effects were observed on the emission spectrum of carboxyfluorescein-labeled S-1 complexed to F-actin used at 2 μM (Figure 7B) or at 30 μM (data not shown). ATP decreased the fluorescence intensity of this S-1 derivative by 20% with a red shift of its emission maximum from 517 to 519 nm whereas the ADP-induced spectrum was similar but not identical to the spectrum of the rigor complex, and its fluorescence profile would reflect a slightly weaker rigor binding of the labeled S-1 to actin. The phosphate analogues ADP·BeFx, ADP·AlF_4, AMP-PNP, or PP_i gave rise to the same spectrum as ATP (data not shown). Such a spectrum was not resulting from turbidity changes consequent on the dissociation state of the rigor complex caused by the γ-phosphate-containing ligands since, as illustrated in Figure 8 for carboxyfluorescein-labeled S-1 and in Figure 6 for EDANS-labeled S-1, the same fluorescence spectrum was also generated by the binding of the γ-phosphate-containing ligands to the labeled S-1 alone. Interestingly, ADP induced the same extent of fluorescence decrease as ATP or the phosphate analogues. However, as observed above (Figures 6 and 7B), actin significantly reduced the ADP effect but not that of the latter ligands most likely because it was less tightly bound to the γ-phosphate-containing nucleotides than to ADP. We conclude that the nucleotide-promoted change in the environment of the fluorophores in the S-1 derivatives complexed or not with F-actin was the manifestation of the predicted conformational cross-talk between the ATPase site

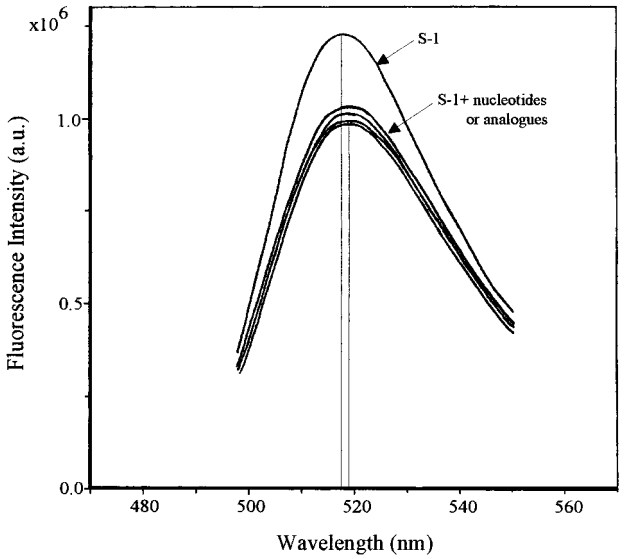

FIGURE 8: Effects of nucleotides or phospate analogues on the fluorescence emission spectrum of [(cysteaminylcarboxyfluorescein)-Cys]S-1. The protein derivative (2 μM) in 50 mM MOPS and 2 mM $MgCl_2$ (pH 7.5) was supplemented with 2 mM ATP, ADP, ADP·BeFx, or ADP·AlF4. Similar spectra were induced by all nucleotides and were slightly displaced for clarity of presentation.

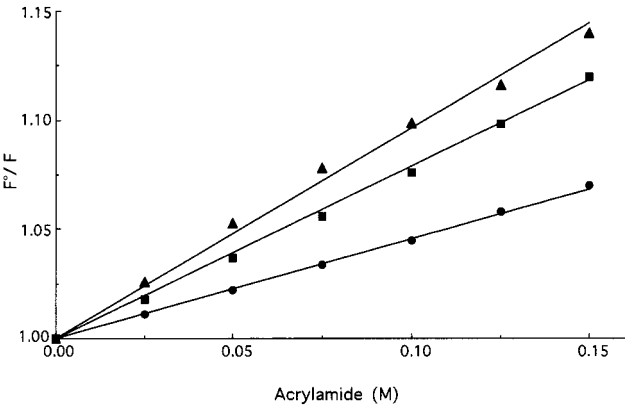

FIGURE 9: Stern−Volmer plots of acrylamide quenching of the fluorescence of [(cysteaminylcarboxyfluorescein)-Cys]S-1. The fluorescence intensities of the labeled protein (1 μM) in 50 mM MOPS and 2 mM Mg Cl_2 (pH 7.5) were measured in the absence (F_0) and presence (F) of the indicated concentrations of the quencher. Fluorescence analyses were performed for the S-1 derivative alone (▲) and for its complexes with F-actin (1 μM) (■) or with ATP (2 mM) (●). The excitation and emission wavelengths were 494 and 519 nm, respectively.

and the actin binding site that modulates the strength of the acto-S-1 interaction.

Finally, we examined the acrylamide quenching of the fluorescence of the [(cysteaminylcarboxyfluorescein)-Cys]S-1 to assess whether the spectral effects caused by F-actin or ATP binding were coupled with a change in the accessibility of the fluorophore to the solvent. The data were analyzed by calculation of Stern−Volmer quenching constants (K_{sv}) from plots in which the initial fluorescence intensity in the absence of acrylamide, F_0, divided by the observed fluorescence in the presence of acrylamide, F, is plotted as a function of the quencher concentration. As shown in Figure 9, all data could be described by a straight line, indicating the presence of a single fluorescent species and the collisional nature of the quenching process. The ability of acrylamide to quench the fluorescence of the label at Cys 540 was weaker than for the free fluorophore within NTB-cysteaminylcarboxyfluorescein ($K_{sv} = 0.93\ M^{-1}$ and $1.49\ M^{-1} \pm 0.05$, respectively), indicating that the probe is embedded in the S-1 structure as suggested above by the particular pattern of the emission spectrum of the S-1 derivative without ligand. Most importantly, F-actin and MgATP affected differently the solvent accessibility. In contrast to F-actin which only modestly decreased the accessibility ($K_{sv} = 0.83\ M^{-1} \pm 0.05$), ATP caused a 2-fold decrease in the solvent exposure of the S-1 fluorophore ($K_{sv} = 0.46\ M^{-1} \pm 0.05$). Thus, ATP and most likely the phosphate analogues share the property to displace the probe to a position that is significantly less accessible to the quencher in the solvent.

DISCUSSION

The synthesis of the two new spectroscopic cysteaminyl mixed disulfides has enabled us to place, via a site-specific labeling reaction, two different extrinsic reporter groups on Cys 540 in the strong actin binding motif of skeletal S-1. The attached EDANS or carboxyfluorescein chromophores have served to accomplish the present fluorescence analyses. But the [(cysteaminyl-Tb^{3+}·DTPA-EDANS)-Cys]S-1 chelate represents also a potentially suitable material for future long distance measurements within S-1 or acto-S-1 by the luminescence resonance energy transfer technique. In this regard, because the substitution of Cys 540 in this chelate does not affect the actin-independent S-1 ATPases, its use would be more convenient for such studies than that of a recently employed derivative of the skeletal myosin motor domain carrying the Tb^{3+}·DTPA chelate bound to Cys 707 whose chemical modification is known to strongly alter the enzymatic activities and mechanical properties of S-1 (*26*). Furthermore, the synthesis procedure we have described makes possible the preparation of other cysteaminyl mixed disulfide analogues including only a different probe, such as an aromatic spin label or a phosphorescent group. This will extend the spectroscopic investigations with the use of electron paramagnetic resonance (EPR) or phosphorescence spectroscopy. The combination of different spectroscopic approaches and labels inserted at a selected site of the interface in a protein complex was recently shown to be valuable for the study of protein−protein interactions (*27*).

The fluorescence emission spectra of the two labels in the corresponding S-1 derivatives and the observed lower extent of carboxyfluorescein S-1 quenching with acrylamide have indicated that both attached fluorophores have established contacts with structural elements of the heavy chain surrounding Cys 540. This observation is consistent with the affinity labeling mechanism of the two mixed disulfide reagents employed that most likely should involve a noncovalent interaction between the cysteaminyl probe side chain and the actin binding site before the specific and efficient modification of Cys 540. The limited exposure to water of the relatively large fluorophore groups is expected to reduce their potential ability to sterically interfer with the access of actin to its strong binding site. This could readily explain the production of only a relatively modest decrease in the rigor acto-S-1 derivative affinity and ATPase rate. Each of the two fluorophores bound to Cys 540 proved to be very sensitive to the strongly bound acto-S-1 complexes. The change in the fluorescence intensity and shift in the emission peak maximum of each S-1 derivative upon rigor binding

of F-actin or F-actin + ADP were clear manifestations of specific conformational states of the strong actin binding motif promoted by these complexes. Distinct fluorescence patterns could be detected for acto-S-1 and acto-S-1−ADP complexes reflecting a tighter rigor interaction of actin with the actin binding motif in the absence than in the presence of ADP and a state change of the motif due to the binding of the latter nucleotide to acto-S-1. Our findings were essentially in agreement with those recently described, using intrinsic fluorescence spectroscopy, for the smooth myosin motor mutant containing a unique tryptophan (W 546) at position 541 of the skeletal S-1 sequence just adjacent to the labeled Cys 540 (*12*). It is noteworthy, however, that while the observed response of this tryptophan consisted mainly of a 7−8 nm blue shift of the emission peak maximum, the fluorescence signal of our two extrinsic labels combined shifts of the maximum emission wavelength and a significant change in the fluorescence intensity. The latter feature allows a quantitative monitoring of the acto-S-1 and acto-S-1−ADP complexes as has been demonstrated with the carboxyfluorescein-labeled S-1. Moreover, it could serve to detect structural differences at the interface between S-1 and actins from different biological sources (*28*). Our data also revealed that the F-actin-induced increase in the hydrophobicity of the microenvironment around Cys 540 was not caused by a decreased exposure of the attached carboxyfluorescein probe to solvent since its fluorescence was only 10% more quenched by acrylamide in the acto-S-1 complex compared to the S-1 derivative alone. Interestingly, earlier, the nitromethane quenching of carboxyfluorescein bound to Lys 553 at the end of the actin binding motif was also found to be unaffected by F-actin binding (*24*, *29*), which does alter the chemical reactivity of this residue (*22*, *24*). Thus, F-actin seems to promote the propagation of a specific structural change along its strong binding motif on S-1 that modifies the polarity of the environment around Cys 540. The proximity of the hydrophobic side chains of the actin helix of residues 338−348 complexed to the motif could also contribute to this polarity change.

Our two extrinsic probes exhibited the additional remarkable property to monitor, in the presence or absence of F-actin, structural changes around Cys 540 elicited by the binding of ATP or the phosphate analogues at the ATPase site located about 75 Å away from Cys 540. These changes seem to be similar for the S-1 derivative dissociated from or weakly bound to F-actin. Therefore, only under experimental conditions promoting a significant production of the weak acto-S-1−nucleotide states could the fluorescence signal serve to specifically identify these particular complexes. Nucleotides are known to induce two major conformational changes within the S-1 catalytic domain; one is located at the cleft separating the upper and lower 50 kDa subdomains and the other at the fulcrum between the catalytic domain and the lever arm domain (*30*). The cleft is part of the actin site, and the labeled Cys 540 is just adjacent to the switch II helix which runs along the cleft and which we have shown to move in solution upon S-1 binding to nucleotides (*20*). Thus, we propose that the associated specific fluorescence change was made possible through the predicted communication from the active site to the actin site of S-1 that determines the crucial dissociation−association properties of the acto-S-1 complex during the contractile cycle (*31*). If so, the nucleotide-dependent fluorescence signal of the probes bound at Cys 540 represents the first spectral evidence for the occurrence in S-1 of this intersite cross-talk. The corresponding fluorescence decrease observed with both labels is useful not only for measuring the binding of nucleotides to S-1 but also for assessing the correct functioning of the intersite communication within various chemically or genetically modified S-1 preparations. Of course, the contribution of a global conformational change in S-1 cannot be directly excluded. However, this possibility is less likely as earlier the nucleotides or phosphate analogues as well as actin were reported to be without influence on the fluorescence emission spectrum of the carboxyfluorescein probe linked to Lys 553 although they did change the chemical reactivity of this amino acid (*24*, *29*). Thus, the effect exerted by nucleotides or analogues on different sites of the strong actin binding motif is not the same, and the region vicinal to Cys 540 appears to be critically involved in the structural transitions induced by these ligands at the strong acto-S-1 interface. The ATP-induced 2-fold decrease of the solvent accessibility of the carboxyfluorescein label bound to Cys 540 suggests that the latter localized conformational rearrangement could cause in solution a reorientation of the partially exposed hydrophobic residues of the motif toward the internal side of S-1, thereby decreasing their interaction with the complementary apolar residues of actin with concomitant reduction of the acto-S-1 affinity.

Additional spectroscopic studies made possible by the two described fluorophores as well as by other probes specifically conjugated to Cys 540 will provide further information and will help to better understand the structural dynamics of the strong actin binding motif throughout the skeletal cross-bridge cycle.

REFERENCES

1. Geeves, M. A. (1991) *Biochem. J. 274*, 1−14.
2. Geeves, M. A., and Conibear, P. B. (1995) *Biophys. J. 68*, 194s−201s.
3. Tsaturyan, A. K., Bershitsky, S. Y., Burns, R., and Fenczi, M. A. (1999) *Biophys. J. 77*, 354−372.
4. Franks-Skiba, K., and Cooke, R. (1995) *Biophys. J. 68*, 142s−149s.
5. Cooke, R. (1997) *Physiol. Rev. 77*, 671−697.
6. Xu, J., and Root, D. D. (1999) *Biophys. J. 76*, 164a.
7. Highsmith, S. (1999) *Biochemistry 38*, 9791−9797.
8. Rayment, I., Holden, H. M., Whittaker, M., Yohn, C. B., Lorenz, M., Holmes, K. C., and Milligan, R. A. (1993) *Science 261*, 58−65.
9. Mendelson, R., and Morris, E. P. (1997) *Proc. Natl. Acad. Sci. U.S.A. 94*, 8533−8538.
10. Milligan, R. A. (1996) *Proc. Natl. Acad. Sci. U.S.A. 93*, 21−26.
11. Fisher, A. J., Smith, C. A., Thoden, J., Smith, R., Sutoh, K., Holden, H., and Rayment, I. (1995) *Biochemistry 34*, 8960−8972.
12. Yengo, C. M., Chrin, L., Rovner, A. S., and Berger, C. L. (1999) *Biochemistry 38*, 14515−14523.
13. Offer, G., Moos, C., and Starr, R. (1973) *J. Mol. Biol. 74*, 653−679.
14. Chaussepied, P., Mornet, D., Audemard, E., Derancourt, J., and Kassab, R. (1986) *Biochemistry 25*, 1134−1140.
15. Eisenberg, E., and Kielley, W. W. (1974) *J. Biol. Chem. 249*, 4742−4748.
16. Bettache, N., Bertrand, R., and Kassab, R. (1989) *Proc. Natl. Acad. Sci. U.S.A. 86*, 6028−6032.
17. Wagner, P. D., and Weeds, A. G. (1977) *J. Mol. Biol. 109*, 455−475.

18. West, J. J., Nagy, B., and Gergely, J. (1967) *J. Biol. Chem. 242*, 1140−1145.
19. Riddles, P. W., Blakeley, R. L., and Zerner, B. (1983) *Methods Enzymol*. *91*, 49−61.
20. Bertrand, R., Capony, J.-P., Derancourt, J., and Kassab, R. (1999) *Biochemistry 38*, 11914−11925.
21. Eftink, M. R., and Ghiron,C. A. (1981) *Anal. Biochem*. *114*, 199−227.
22. Bertrand, R., Derancourt, J., and Kassab, R. (1995) *Biochemistry 34*, 9500−9507.
23. Bertrand, R., Derancourt, J., and Kassab, R. (1997) *Biochemistry 36*, 9703−9714.
24. Peyser, Y. M., and Muhlrad, A. (1999) *Eur. J. Biochem*. *263*, 511−517.
25. Chen, J., and Selvin, P. R. (1999) *Bioconjugate Chem*. *10*, 311−315.
26. Getz, E. B., Cooke, R., and Selvin, P. R. (1998) *Biophys. J. 74*, 2451−2458.
27. Owenius, R., Osterlund, M., Lindgren, M., Svensson, M., Olsen, O. H., Persson, E., Freskgard, P.-O., and Carlsson, U. (1999) *Biophys. J. 77*, 2237−2250.
28. Prochniewicz, E., and Thomas, D. D. (1999) *Biochemistry 38*, 14860−14867.
29. MacLean, J. J., Chrin, L. R., and Berger, C. L. (2000) *Biophys. J. 78*, 1441−1448.
30. Highsmith, S. (1999) *Biochemistry 38*, 9791−9797.
31. Morales, M. F., and Botts, J. (1979) *Proc. Natl. Acad. Sci. U.S.A. 76*, 3857−3859.

BI000834U